International Journal of Nanomedicine

Dovepress
open access to scientific and medical research

Open Access Full Text Article

ORIGINAL RESEARCH

Accurately Controlled Delivery of Temozolomide by Biocompatible UiO-66-NH_2 Through Ultrasound to Enhance the Antitumor Efficacy and Attenuate the Toxicity for Treatment of Malignant Glioma

Zhiping Wan[1,*]
Chunlin Li[2,*]
Jinmao Gu[1,*]
Jun Qian[1]
Junle Zhu[1]
Jiaqi Wang[2]
Yinwen Li[2]
Jiahao Jiang[1]
Huairui Chen[1]
Chun Luo[1]

[1]Department of Neurosurgery, Tongji Hospital, School of Medicine, Tongji University, Shanghai, 200092, People's Republic of China; [2]Trauma Center, Shanghai General Hospital, Shanghai Jiao Tong University School of Medicine, Shanghai, People's Republic of China

*These authors contributed equally to this work

Background: Glioma is the most common and malignant primary brain tumour in adults and has a dismal prognosis. Temozolomide (TMZ) is the only clinical first-line chemotherapy drug for malignant glioma up to present. Due to poor aqueous solubility and toxic effects, TMZ is still inefficient and limited for clinical glioma treatment.

Methods: UiO-66-NH_2 nanoparticle is a zirconium-based framework, constructed by Zr and 2-amino-1,4-benzenedicarboxylic acid (BDC-NH_2) with octahedral microporous structure, which can be decomposed by the body into an ionic form to discharge. We prepared the nanoscale metal-organic framework (MOF) of UiO-66-NH_2 to load TMZ for therapy of malignant glioma, TMZ is released from UiO-66-NH_2 through a porous structure. The ultrasound accelerates its porous percolation and promotes the rapid dissolution of TMZ through low-frequency oscillations and cavitation effect. The biological safety and antitumor efficacy were evaluated both in vitro and in vivo.

Results: The prepared TMZ@MOF exhibited excellent biocompatibility and biosafety due to minimal drug leakage without ultrasound intervention. We further used the flank model of glioblastoma to verify the in vivo therapeutic effect. TMZ@UiO-66-NH_2 nanocomposites could be well delivered to the tumour tissue, which led to local enrichment of the TMZ concentration. Furthermore, TMZ@UiO-66-NH_2 nanocomposites under ultrasound demonstrated much more efficient inhibition for tumor growth than TMZ@UiO-66-NH_2 nanocomposites and TMZ alone. Meanwhile, the bone marrow suppression side effects of TMZ were significantly reduced by TMZ@UiO-66-NH_2 nanocomposites.

Conclusion: In this work, TMZ@UiO-66-NH_2 nanocomposites with ultrasound mediation could effectively improve the killing effect of malignant glioma and decrease TMZ-induced toxicity in normal tissues, demonstrating great potential for the delivery of TMZ in the clinical treatment of malignant gliomas.

Keywords: MOF, TMZ, ultrasound glioma

Introduction

The prognosis is extremely poor for malignant gliomas, especially glioblastoma (GBM), which account for approximately 47.7% of brain malignant tumours.[1] At present, the main treatment protocol is surgical adjuvant radiotherapy and chemotherapy. Postoperative temozolomide (TMZ) adjuvant chemotherapy is a common clinical treatment among the few available treatments for glioblastoma. However, it lacks

Correspondence: Chun Luo; Huairui Chen
Email boyluochun@126.com; chen13761626536@163.com

Received: 26 July 2021
Accepted: 22 September 2021
Published: 9 October 2021

selectivity and has an insufficient brain tumour focal concentration, which leads to very limited therapeutic effect and causes a series of side effects in clinical applications. Among these side effects, haematopoietic suppression has become the most severe problem associated with TMZ.[2] Thus, it is necessary to develop a new strategy to precisely deliver and release TMZ in the tumour region.

With the rapid development of nanotechnology, organic and inorganic delivery nanocarriers, such as inorganic nanoparticles, liposomes, polymeric nanoparticles and so on, have been widely used as selective delivery of drugs in the treatment of tumours.[3] In recent years, MOFs have been widely developed as vehicles for effective delivery of drugs to tumour tissues. MOFs is a new class of crystalline porous materials constructed by metal ions/clusters and organic linkers.[4] Due to internal circulation stability, high loading capacity, and excellent biocompatibility, MOFs provide an unprecedented opportunity for the treatment of cancer.[5] Especially, the nanoscale MOF of UiO-66-NH_2 can be as an ideal drug-delivery nanoparticle because it has superior cavity volume and slow-release functions,[6] which is expected to penetrate the blood–brain barrier (BBB). UiO-66-NH_2 nanoparticle is a zirconium-based framework constructed by Zr and 2-amino-1,4-benzenedicarboxylic acid (BDC-NH2) with octahedral microporous structure, exhibiting great chemical and thermal stability.[4] To design MOF nanocomposites as carriers for controllable drug release, various factors such as hydrophobicity, pH, temperature, biomolecular reactions, light and ultrasound are considered.[7] Among them, ultrasound-mediated targeted drug delivery has shown excellent properties for pinpointing the location, penetration, and controllable energy.[8]

Ultrasound has been shown to be effective in strengthening drug transport into tissues. The use of low-energy focused ultrasound mediated BBB disruption is an emerging new technology, which makes use of the physical interactions between ultrasonic waves and systemically drug-loaded nanoparticles to transiently disrupt the BBB.[9] This technique has been used to enhance the delivery of chemotherapeutic agents in ultrasound-targeted regions of the brain.[10] Preclinical and clinical studies have demonstrated that ultrasound-mediated BBB disruption is well tolerated in both animal models and humans.[11,12] In regard to glioma, the ultrasound-mediated targeted delivery and distribution of polymeric nanoparticles has great application potential. Conventional ultrasound-directed approaches mainly use microbubbles, such as liposomes, as carriers.[13] TMZ is released from UiO-66-NH2 through a porous structure. Ultrasound accelerates its porous percolation and promotes the rapid dissolution of TMZ through low-frequency oscillations and cavitation effect.[9] UiO-66-NH2 is very stable and hard for physical disruption, but it can be decomposed by the body into an ionic form to discharge. In addition, the use of low-energy focused ultrasound also can disrupt the blood–brain barrier to enhance the drug delivery into the glioma site.[14] However, MOFs as drug delivery systems are rarely reported in ultrasound-mediated targeted approaches.

Herein, UiO-66-NH_2 nanocomposites were prepared for delivery of TMZ, which could be effectively delivered to the tumour tissue. When combined with ultrasound intervention, TMZ was dramatically and rapidly released at the tumor site to achieve an enhanced antitumor effect (Scheme 1). Moreover, this method reduced the release of drug in normal tissues and then decreased side effects. Our study demonstrated the potential of using TMZ@UiO-66-NH_2 as a drug carrier in ultrasound-mediated targeted approaches.

Materials and Methods

Materials

Temozolomide (TMZ) was purchased from Wuhan Yuancheng Technology Development Co. Ltd, China. The Cell Counting Kit-8 (CCK-8) and Terminal-deoxynucleotidyl Transferase Mediated Nick End Labeling (TUNEL) assay kit were purchased from Yeasen Biological Technology, Shanghai, China, and Abcam, USA, respectively. The primary antibodies were obtained from Cell Signaling Technology, USA, and the secondary antibodies were purchased from LI-COR, USA. Water and all buffers were pretreated with Chelex 100 resin so that there were no heavy metals in the aqueous solution. All other chemical reagents and reaction buffers were purchased from Sinopharm Chemical Reagent, China.

Synthesis and Characterization of UiO-66-NH_2 Nanoparticles

UiO-66-NH_2 nanoparticles were prepared according to the previous method.[15] For this, 0.24 g of $ZrCl_4$ were dissolved in 60 mL of DMF, then 0.186 g of 2-amino-1,4-benzenedicarboxylic acid (BDC-NH_2) and 0.15mL of deionized water were added to the above solution. Then the mixture were transferred to a 100-mL hydrothermal reactor and reacted for 24 h at 120°C in an oven. Finally, the UiO-66-NH_2 were obtained after washing and freeze-drying. The morphology of the UiO-66-NH_2 was measured by transmission electron microscopy (TEM, JEM-2100F).

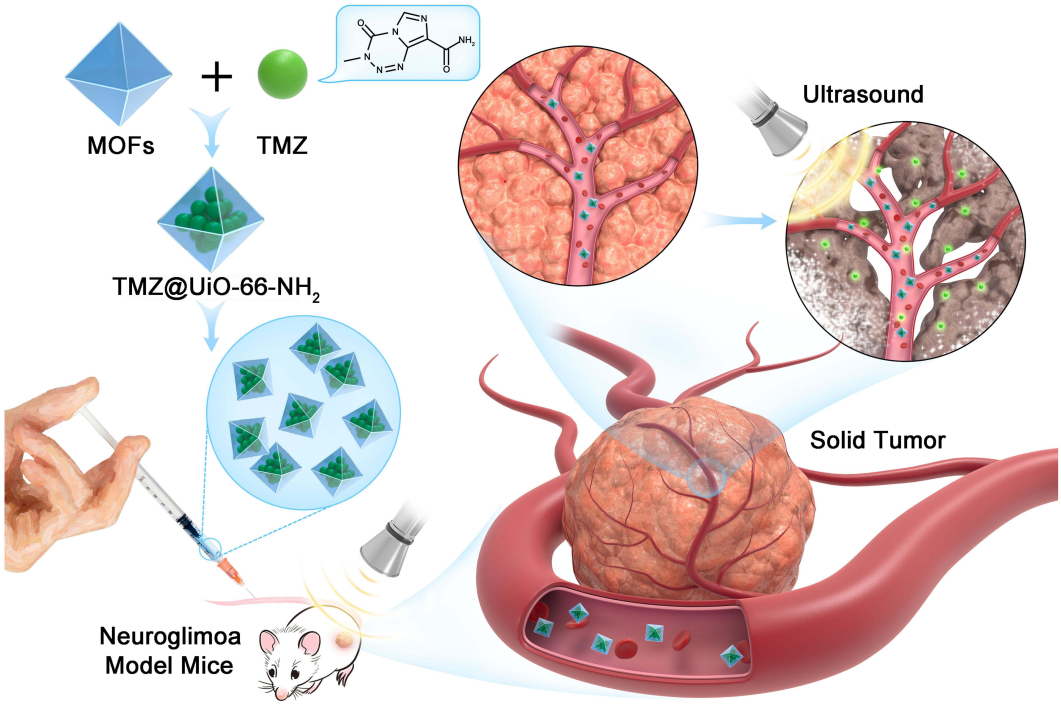

Scheme 1 Schematic diagram of the concept of ultrasound-controlled biocompatible TMZ@UiO-66-NH_2 nanocomposites drug delivery system.

In vitro Experiment

Drug Loading and Release

A total of 5.0 mg of UiO-66-NH_2 nanoparticles were mixed with 10 mL of TMZ (Wuhan Yuancheng Technology Development Co. Ltd, China) and water solution at a concentration of 50 μg/mL. At room temperature, the mixture was shaken for 36 hours under dark conditions to obtain a balanced solution. The TMZ-loaded UiO-66-NH_2 nanocomposites (TMZ@UiO-66-NH_2) were collected by centrifugation and washed with deionized water twice to remove unbound TMZ. The concentration of free TMZ in the collected supernatants was determined using a UV-Vis-NIR spectrophotometer with the absorbance at 330 nm. The TMZ loading efficiency was calculated by the following equation: loading efficiency = ((weight of loaded TMZ)/(weight of nanocomposites and loaded TMZ)) × 100%.

The release of TMZ from the TMZ@UiO-66-NH2 nanocomposites with ultrasound irradiation by a ultrasonic apparatus (Topteam161 Physioson-Basic, Physioson Elektromedizin AG, Germany) (1 MHz pulsed ultrasound with 100 Hz pulse repetition frequency, 1:5 duty cycle, and 1.0 MPa peak rarefactional pressure). 5.0 mg of TMZ@UiO-66-NH2 nanocomposites were dispersed in 5.0 mL of PBS (Phosphate Buffer Saline) solutions at physiological pH (pH~7.4) and serum, respectively. The mixture was treated by consecutive ultrasonic at room temperature and the dispersions were collected after 0, 1, 2, 4, 8, 16 and 24 min to collect the supernatants by centrifugation at 2000 rpm for 15 min. Then, the concentration of TMZ was determined as before. Drug release percentage was calculated by $C_t/C_{max}\times100$. C_t and C_{max} represent the TMZ concentration at the time t, and the maximum concentration of TMZ that can be released, respectively. Finally, the percentage of TMZ released from TMZ@UiO-66-NH_2 was plotted against time.

Cell Culture Studies

Glioma cells of U251, BMSCs, HUVECs, SHG44 and U87 were purchased from the American Type Culture Collection (ATCC, Rockville, MD, USA). All these cell lines were authenticated twice by morphologic and isoenzyme analyses during the study period. Cell lines were routinely checked for mycoplasma using Hoechst staining to indicate contamination, which was consistently found to be negative. All the cells mentioned above were cultured in DMEM high-glucose medium (4.5 g/L, Gibco, NY, USA), which was supplemented with 10% fetal bovine serum (FBS, Gibco, NY, USA), 100 U/mL penicillin and 100 U/mL streptomycin (Thermo Fisher Scientific, Multiskan GO, Waltham, MA, USA) at PH 7.4. All cells were cultured in a humidified incubator with 5% CO_2 at

37°C. For the passage of cells mentioned above, we treated cells with 2 mL of 0.25% trypsin containing 0.02% EDTA (Grand Island, New York, USA) for 1 min at 37°C when the cultures were almost 80% confluent. And we harvested cells with 0.25% trypsin containing 0.02% EDTA in their logarithmic growth phase for the following experiments.

Cell Proliferation Assay

We determined the inhibitory effect on U251, BMSCs, HUVECs, SHG44 and U87 to evaluate the in vitro safety of TMZ, UiO-66-NH2 and TMZ@UiO-66-NH2. U251and SHG44 malignant glioma cell lines were seeded at a density of 5000 cells per well in a flat-bottomed 96-well plate for 24 h in a humidified 37°C and 5% CO_2 atmosphere. After 24 h, the cells were incubated with an increasing concentration of TMZ (ranging from 0 to 87.4 μg/mL), or TMZ@UiO-66-NH2 (ranging from 0 to 0.45 mg/mL) or TMZ@UiO-66-NH2 (ranging from 0 to 0.45 mg/mL, TMZ loading content was 0.241mg TMZ/mg UiO-66-NH2). The cells of US treatment were treated with ultrasound (1 MHz pulsed ultrasound with 100 Hz pulse repetition frequency, 1:5 duty cycle, and 1.0 MPa peak rarefactional pressure) for 1min immediately and at 24 h, 48 h later, cell proliferation was determined by the CCK-8 (Yeasen Biological Technology, Shanghai, China) according to the manufacturer's instructions, and the results were read using a microplate reader.

Transwell Assays

We used 24-well transwell chambers with 8 μm nitrocellulose pore filters (Costar, Transwell, Corning, New York, NY, USA) to evaluate the effect of the TMZ, TMZ@UiO-66-NH_2 and TMZ@UiO-66-NH_2 + ultrasound on the migration of U251 and SHG44 cells. Cells were divided into four groups: the control group, the TMZ group, TMZ@UiO-66-NH_2 group and TMZ@UiO-66-NH_2 + ultrasound group. The cells in control group was resuspended in serum-free medium, the cells in TMZ group was resuspended in serum-free medium containing the TMZ at a concentration of 77.7 μg/mL, the cells in TMZ@UiO-66-NH_2 group was resuspended in serum-free medium containing the TMZ@UiO-66-NH_2 at a concentration of 0.4 mg/mL (TMZ loading content was 0.241mg TMZ/mg UiO-66-NH2), the cells in TMZ@UiO-66-NH_2 + ultrasound group was resuspended in serum-free medium containing the TMZ@UiO-66-NH_2 at a concentration of 0.4mg/mL and treated with ultrasound (1 MHz pulsed ultrasound with 100 Hz pulse repetition frequency, 1:5 duty cycle, and 1.0 MPa peak rarefactional pressure) for 1min. Then, the cells were loaded into the upper chamber, and medium containing 10% FBS was placed in the lower chamber for 48h. Finally, we fixed cells that passed through the membranes of the upper chambers with 4% paraformaldehyde (Servicebio, Wuhan, Hubei, China) and stained with 1% crystal violet dye solution (Beyotime Biotechnology, Shanghai, China).

Analysis of Cell Apoptosis

We seed U251 and SHG44 cells in 6-well plates and divided these cells into four groups: the control group, the TMZ group (TMZ at a concentration of 77.7 μg/mL), TMZ@UiO-66-NH_2 group (TMZ@UiO-66-NH_2 at a concentration of 0.4 mg/mL) and TMZ@UiO-66-NH_2 + ultrasound group (TMZ@UiO-66-NH_2 at a concentration of 0.4 mg/mL and treated with ultrasound for 1min. The physical parameters were 1 MHz pulsed ultrasound with 100 Hz pulse repetition frequency, 1:5 duty cycle, and 1.0 MPa peak rarefactional pressure). After 48 hours, we detected the apoptosis of U251 and SHG44 cells using Annexin V-FITC/PI Kit (Invitrogen, Waltham, MA, USA) and TUNEL Kit (Yeasen Biological Technology, Shanghai, China). For the Annexin V-FITC/PI assay, U251 and SHG44 cells were washed with PBS and binding buffer three times and resuspended in 200 μL of binding buffer, then we added 10 μL of Annexin V-FITC into the cell suspension and stained for around 15 min on ice in the dark. Finally, PI was added to the binding buffer and the cells were stained for 5 min before analyzing the flow cytometry (BD, AccuriTM C6, Franklin Lakes, NJ, USA). For the TUNEL assay, U251 and SHG44 cells were fixed with 4% paraformaldehyde and permeabilized with TritonX-100 (Beyotime Biotechnology), after washed three times with PBS, 50 μL of TUNEL reaction mixture were added into the reaction mixture according to the manufacturer's instructions. Finally, we stained the nuclei with DAPI (Yeasen Biological Technology, Shanghai, China) and observed them under a fluorescence microscope (Leica, Leica DMi8).

Cell Cycle Analysis

The methods to set up the experimental group and control group were the same as those mentioned above. U251 and SHG44 cells were harvested with 0.25% trypsin containing 0.02% EDTA in their logarithmic growth phase, washed three times in PBS and then stained with 5 μL PI

(BD, Franklin Lakes, NJ, USA) for 30 min on ice in the dark. Then, the distribution of the cell cycle was analysed by flow cytometry.

Western Blot Assay

The methods to set up the experimental and control groups were the same as those mentioned above. After the required treatment period, U251 and SHG44 cells were washed three times with PBS and then lysed in lysis buffer (Biotech Well, Shanghai, China) containing protease inhibitors (Biotech Well, Shanghai, China), phosphatase inhibitors (Biotech Well, Shanghai, China) and phenylmethanesulfonyl fluoride (PMSF) (Biotech Well, Shanghai, China). Next, a bicinchoninic acid (BCA) protein assay kit (Biotech Well, Shanghai, China) was used to determine the protein concentration. Equal amounts of protein from each group were electrophoresed in place and then transferred to a cellulose acetate membrane. The antibody dilutions of MMP-2, MMP-9, MMP-13, Bax, Bcl-2, Cleaved Caspase-3 and β-actin was 1:1000, 1:1000, 1:3000, 1:1000, 1:1000, 1:1000 and 1:3000, respectively. The cellulose acetate membrane was then incubated with primary antibodies including anti-MMP-2, anti-MMP-9, anti-MMP-13 (Abcam, Cambridge, UK), anti-cleaved caspase-3, anti-Bax, anti-Bcl-2 (Cell Signaling Technology, Danvers, MA, USA) and anti-β-actin (Proteintech, Wuhan, Hubei, China) at 4°C overnight after blocking in 5% nonfat milk (Sangon Biotech, Shanghai, China) for 2 hours with rocking. Finally, after incubation with the corresponding secondary antibodies including goat anti-mouse IgG (H + L) and goat anti-rabbit IgG (H + L) (LI-COR, Lincoln, NE, USA) at room temperature for 2 hours, we detected the protein with fluorography (LI-COR, Odyssey CLX, Lincoln, NE, USA).

In vivo Studies

All experiments were approved by the Experimental Animal Center of Shanghai Jiao Tong University. Four-week-old male BALB/c nude mice were bred and maintained under a 12/12 hours light/dark cycle with free access to food and water. The temperature was maintained at around 20°C, and the relative humidity was set to around 50%. The mice for in vivo experiments were conducted following the protocols of Shanghai Committee for the Accreditation of Laboratory Animal. All processes have been approved by Shanghai Science and Technology Commission (the Laboratory Animal Use Permit Number: SYXK2019-0005. Shanghai, China). All the operations were performed after sodium pentobarbital anesthesia with all efforts made to minimize the suffering of mice.

To establish xenograft neuroglioma model mice, U87 cells (1×10^7 in 100μL of PBS per mouse) were implanted subcutaneously into the dorsal flank of each mouse. When the tumour volume reached an average of approximately 200mm^3, animals were randomly distributed into four groups: control group, TMZ group (TMZ 25 mg/kg i.p. every 2 days for 4 weeks), TMZ@UiO-66-NH_2 group (TMZ@UiO-66-NH2 125 mg/kg i.p. every 2 days for 4 weeks, TMZ loading content was 19.4 wt%) and TMZ@UiO-66-NH_2 + ultrasound group (TMZ@UiO-66-NH_2 125 mg/kg i.p. every 2 days and treated with ultrasound for 15 min every day for 4 weeks, TMZ loading content was 19.4 wt%). Ultrasound was focused in and around the tumor and the physical parameters were 1 MHz pulsed ultrasound with 100 Hz pulse repetition frequency, 1:5 duty cycle, and 1.0 MPa peak rarefactional pressure. Tumors of mice were measured with vernier caliper every 3 days after the first treatment and the volume of the tumors were calculated with the formula: volume (mm^3) = (length × $width^2$)/2. Four weeks after treatment, the mice were killed and the tumor samples were collected for the following analyses.

Analysis of Myelosuppression and Hepatic Function

Four-week-old male BALB/c nude mice were randomly distributed into three groups: control group, TMZ group (TMZ 100 mg/kg i.p. every days for 4 weeks), TMZ@UiO-66-NH_2 group TMZ@UiO-66-NH_2 500 mg/kg i.p. every days for 4 weeks and TMZ@UiO-66-NH_2 + ultrasound group TMZ@UiO-66-NH_2 500 mg/kg i.p. every days and treated with ultrasound for 15min every day for 4 weeks. Ultrasound was focused in and around the tumor and the physical parameters were 1 MHz pulsed ultrasound with 100 Hz pulse repetition frequency, 1:5 duty cycle, and 1.0 MPa peak rarefactional pressure. Whole-blood samples and serum of mice from different groups were collected via the ophthalmic vein and centrifuged (5000 rpm, 15 min, 4°C). WBC (white blood cell), lymph (lymphocyte), HGB (hemoglobin), PLT (platelet), ALT (alanine aminotransferase) and AST (aspartate aminotransferase) were measured.

Haematoxylin and Eosin (HE) Staining Assay

The liver, heart, spleen, lung, kidney tissues obtained from mice were fixed with 4% formaldehyde and cut into 4μm sections after embedded in paraffin. Then, the sections

were baked for 4 hours at 70°C. After dewaxed and hydrated in distilled water, the sections were stained with haematoxylin and then counterstained with eosin. And the sections were dehydrated with ethanol and transparentized with xylene I and xylene II before being observed under a microscope (Leica, Leica DMi8) assess histological alterations.

Immunohistochemistry Assay

The tumor tissue obtained from different groups were fixed with 4% formaldehyde and cut into 4 μm sections to mounted on microscopic slides after embedded in paraffin. Then, the specimens were deparaffinized, rehydrated, and incubated with primary antibody at 4°C overnight, followed by 1h incubation of secondary antibody at room temperature. Finally, we adopted the avidin biotinylated peroxidase complex methods to determine the expression of target protein so that we can observe and assess histological alterations under a microscope. The positive stained integrated optical density (IOD) of different groups was measured using the ImageJ software (National Institutes of Health, Bethesda, MD, USA).

Statistical Analysis

All experiments were performed at least three times. Quantitative or semiquantitative data were expressed as means ± standard error of the mean (SD). All statistical data were analyzed using GraphPad Prism 6 (GraphPad Software Inc, La Jolla, CA, USA). The differences of data between two groups were determined by two-tailed unpaired or paired *t*-tests and multiple groups were compared by ANOVA followed by Tukey's posttests. The differences were considered statistically significant at a P value <0.05.

Results and Discussion

UiO-66-NH_2 was constructed by Zr and 2-amino-1,4-benzenedicarboxylic acid (BDC-NH_2) with octahedral structure (Figure 1A). The TEM images of TMZ@UiO-66-NH_2 nanocomposites further showed octahedral morphology and a diameter of ~90 nm (Figure 1B and C), which allowed them to effectively penetrate the tumour tissue or even the blood–brain barrier.[16] The UiO-66-NH2 MOFs were also measured by dynamic light scattering (DLS) method (Malvern ZS90). The UiO-66-NH2 MOFs have a mean size of ~150 nm (Figure S1), and their zeta potential is ~9.8 mV. The XRD patterns well match with the typical peaks of (111), (002) and (006) crystal planes of UiO-66-NH_2 (Figure 1D),[4,15,17] proving successful synthesis of the nanomaterials. The XRD patterns also according to other research about the UiO-66-NH_2. The Fourier transform infrared (FTIR) spectra of UiO-66-NH_2 shows adsorption bands at 1381 cm^{-1} and 1257 cm^{-1}, which correspond to the C–N stretching vibration. The adsorption bands at 1569 cm^{-1} and 3442 cm^{-1} are assigned to the OCO asymmetric stretching vibration and asymmetric N-H stretching vibration (Figure 1E)[4,18] respectively. These results confirmed that UiO-66-NH_2 have been successfully prepared. On account of its large internal pore volumes, the UiO-66-NH2 had loading capacities of above 0.25 mg TMZ/mg UiO-66-NH_2. The TMZ hardly released in PBS (pH 7.4) and serum at 37°C (Figure 1F and G), which confirmed very low side effect for normal tissue. These results can be attributed to low solubility of temozolomide[19] and high pore volumes, slow dissolution release structure of porous UiO-66-NH_2.[20] To target glioma in the brain and increase the drug concentration, ultrasound has been extensively explored in glioma therapy.[21,22] Ultrasound-controlled drug delivery systems have capabilities of high penetration, real-time observation, noninvasive methodology, high efficiency, ease of energy control, low cost and high safety.[13,23] Recent studies have shown that high-intensity focused ultrasound can be used to transiently disrupt the blood–brain barrier without damaging the surrounding neural tissue.[24,25] The TMZ released very rapidly under the ultrasound mediation both in in PBS (pH 7.4) and serum, after 24 min, almost all the TMZ have released from the TMZ@UiO-66-NH_2 nanocomposites. The ultrasound-mediated targeted drug delivery is very beneficial for therapy of glioma to enhance treatment effect and reduce side effect.

We have used two typical normal cells (BMSCs and HUVEC cells) to elevate the biocompatibility of the UiO-66-NH_2. The UiO-66-NH_2 exhibited good biocompatibility for normal cells; even at the concentration of 450 μg/mL (Figure 1H and I), there were still no appreciable adverse effect for the cells survival. The results indicated that UiO-66-NH_2 had good biosafety. We also studied the viability of BMSCs, HUVECs, SHG44 and U251 cells to detect the background toxicity of empty MOFs under ultrasound. The results showed that there are no significant adverse effects of ultrasound treatment (Figure S2). To verify the cytotoxicity of TMZ and TMZ@UiO-66-NH_2 nanocomposites in U251 and SHG44 cells, CCK-8 assays were conducted (Figure 1J and K). The TMZ effectively decreased the malignant glioma cell viability, while the

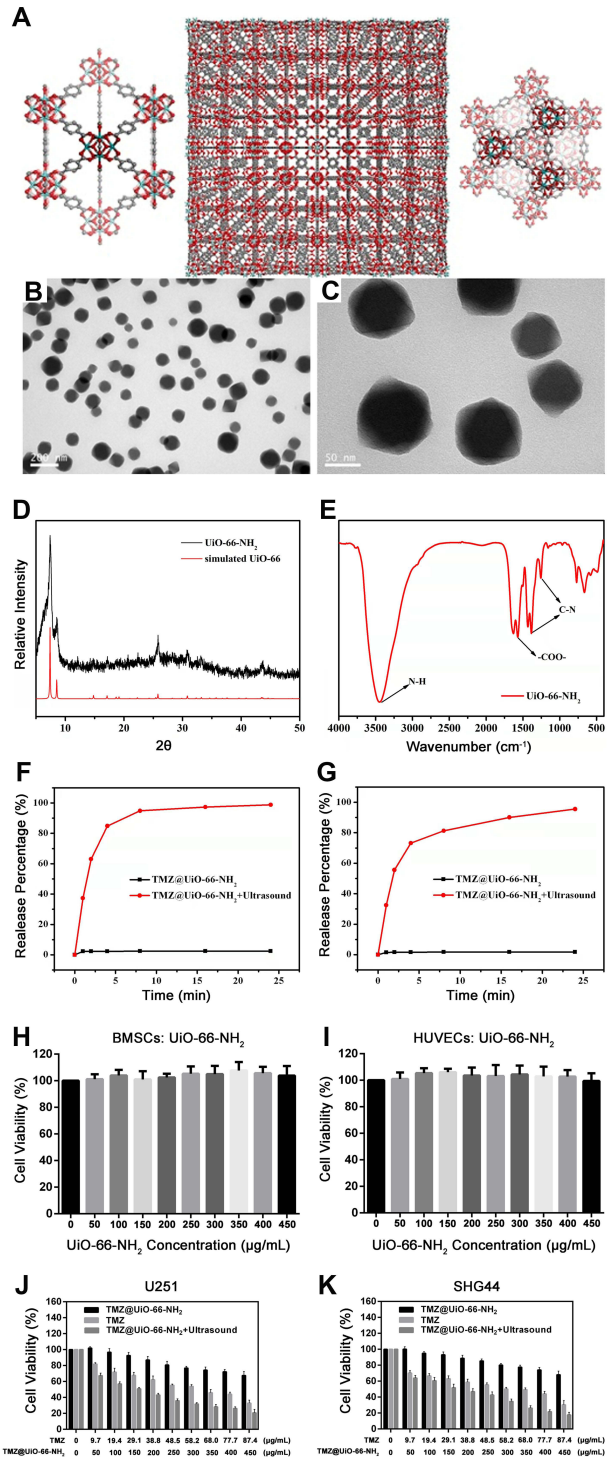

Figure 1 Characterization and cytotoxicity of the TMZ@UiO-66-NH_2 nanocomposites. (**A**) Organic–inorganic hybridization structure of TMZ@UiO-66-NH_2. (**B**) Low- and (**C**) high-magnification TEM image of the TMZ@UiO-66-NH_2. (**D**) The XRD patterns and (**E**) Fourier transform infrared (FTIR) spectra of UiO-66-NH_2. The cumulative release of TMZ from the TMZ@UiO-66-NH_2 in (**F**) PBS and (**G**) serum before and after ultrasound for 0, 1, 2, 4, 8, 16 and 24 min. The cell viabilities of (**H**) BMSCs and (**I**) HUVEC cells incubated with the UiO-66-NH_2 for 24 h. The cell viability of (**J**) U251 and (**K**) SHG44 cells incubated with different concentrations of the TMZ@UiO-66-NH_2, TMZ or TMZ@UiO-66-NH_2+Ultrasound for 48 h. At each concentration point, the loaded TMZ in UiO-66-NH_2 had same concentration as free TMZ. Data are expressed as means ± SDs (n=3).

Abbreviations: TEM, transmission electron microscopy; XRD, X-ray diffraction; FTIR, Fourier transform infrared; TMZ, temozolomide; PBS, phosphate-buffered saline; BMSCs, bone mesenchymal stem cells; HUVECs, human umbilical vein vessel endothelial cells; MOF, metal organic frameworks.

TMZ@UiO-66-NH_2 group showed limited inhibition of tumour cell viability due to its insufficient release of TMZ. These phenomenon may lead to the poor glioma chemotherapy effects and drug resistance. However, TMZ@UiO-66-NH_2 could effectively depressed the malignant glioma cell viability with ultrasound intervention, which was similar to free TMZ. These results could be attributed to rapid and accurate release of TMZ under ultrasound intervention. Therefore, to rapidly and accurately increase the TMZ concentration in local tumour tissue, ultrasound intervention is an effective way for treatment of glioma.

Glioma migration plays an important role in tumor progression, Zhou et al demonstrated that glioma migration was closely related to tumour recurrence and clinical prognosis.[26] In the present study, Transwell assays were conducted to detect the capability of glioma cell migration and invasion. Therefore, we evaluated the migration inhibition of U251 and SHG44 cell lines in each group. When combining TMZ@UiO-66-NH_2 nanocomposites with ultrasound intervention, the tumours were significantly suppressed, showing that both TMZ and TMZ@UiO-66-NH_2 + Ultrasound could play an effective role in the inhibition of glioma cell transfer ability. The burst release of TMZ may have contributed to the observed anti-tumour efficacy, which is considered a suppressor in glioma migration.[27] When TMZ@UiO-66-NH_2 was combined with ultrasound intervention, tumour migration inhibition was obvious and even more potent than TMZ alone (Figure 2A–C), which could be explained by one of two mechanisms: destruction of the carrier to release the physically trapped drug,[28] or structural changes in cells and tissues to promote the targeted release of therapeutic substances to local tumours.[29] This work demonstrated that ultrasound intervention-based disruption of the BBB may be an effective technique to enhance the penetration of TMZ in glioma. Nevertheless, malignant glioma cell migration was not inhibited in the TMZ@UiO-66-NH_2 group, possibly due to the insufficient release of drugs after drug loading into UiO-66-NH_2 nanomaterials. Moreover, tumour migration is an important cause of tumour refractoriness. A previous study demonstrated that the downregulation of matrix metalloproteinases (MMPs) expression in glioma cells significantly decreases their migration and invasiveness[30,31] and TMZ can substantially inhibit the migration of glioma cells in vitro.[32] MMPs, protein bio-markers that represent tumour migration and invasion,[33] were detected to analyse the degree of migration. Therefore, we detected MMP-2, MMP-9 and MMP-13 expression through Western blot experiments (Figure 2D and E). TMZ group and TMZ@UiO-66-NH_2 +Ultrasound groups showed decreased expression. Compared to the control group or TMZ group in both cells, MMP-2 and MMP-9 expression were efficiently suppressed in TMZ@UiO-66-NH2 +Ultrasound group (Figure 2F, G, I and J). But TMZ@UiO-66-NH2 group was not statistically significant compared to the control group, and the reason should be associated with insufficient local release concentrations of TMZ. For MMP-13, the expression volume was significantly reduced alike in TMZ@UiO-66-NH2 +Ultrasound group (Figure 2H and K). In general, when compared with the TMZ group and TMZ@UiO-66-NH_2 group, the TMZ@UiO-66-NH_2 +Ultrasound group had a stronger inhibition ability of migration-related protein expression (Figure 2F–K). According to the results, TMZ increased in TMZ@UiO-66-NH2 and played an important role in inhibiting malignant glioma cells' migration, possibly by regulating the AMPK-TSC-mTOR signaling pathway to suppress the expression of MMP.[34] Additionally, the inhibition ability was related to TMZ concentration, which explained the low MMP expression in the TMZ@(UiO-66-NH_2) group. When further combined with ultrasound-mediated targeted intervention, it quickly boosted the targeted regional drug concentration, thus enhancing the role of glioma cell growth and invasiveness suppression. Daniel Y Zhang et al mentioned that ultrasound may enhance anti-tumour effect by increasing the sensitivity of glioblastoma to chemotherapeutic agents,[9] which explained TMZ@UiO-66-NH_2 +Ultrasound group performed better in inhibiting malignant glioma cells' migration and suppressing the expression of MMP than TMZ alone. But the specific underlying mechanisms require further validation.

Inducing apoptosis is an important way to induce glioma cell death. Karpel-Massler et al elicited a nuclear stress response through inhibition of PARP-1 in malignant glioma cells, which included the upregulation of downstream DNA stress response proteins and enhanced TRAIL-mediated apoptosis in glioma cells.[35] Das et al also demonstrated that a decrease in the Bax/Bcl-2 ratio caused by dexamethasone significantly attenuated TMZ-induced apoptosis in cultured U87MG glioma cells.[36] The anti-tumour effect of temozolomide mainly promotes DNA fragmentation and apoptosis of malignant glioma cells. To test the in vitro cytotoxic effect, both flow cytometry (Figure 3A) and TUNEL (Figure 3D) assays were

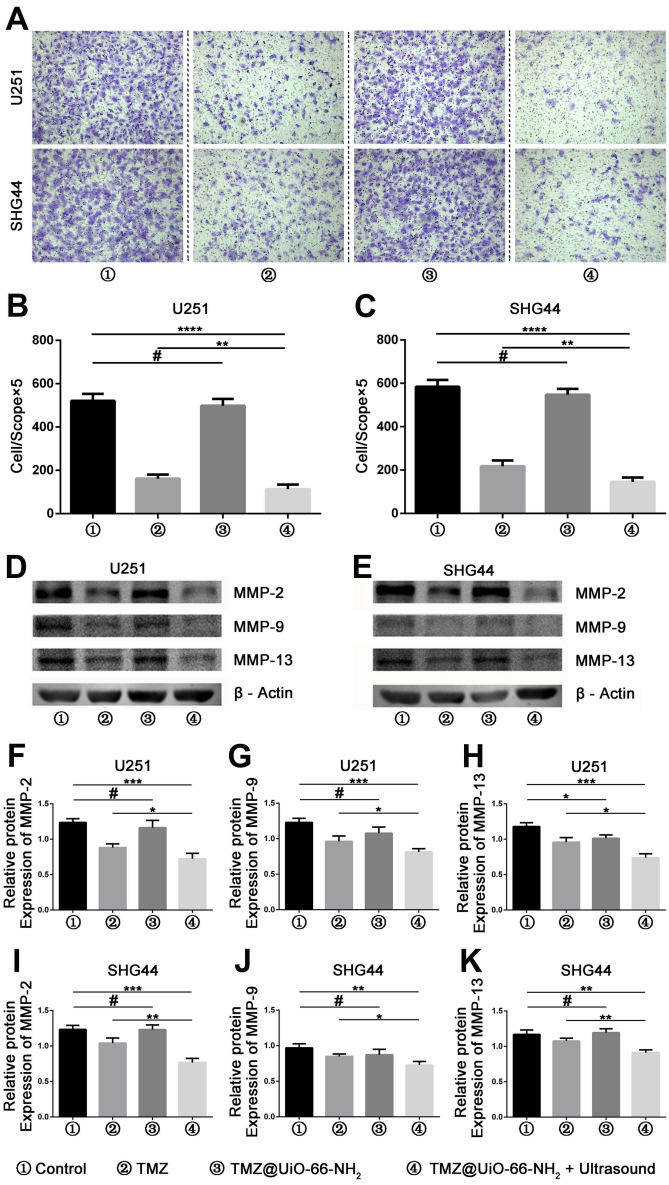

Figure 2 TMZ@UiO-66-NH_2 + ultrasound inhibited the malignant biological behaviors of U251 and SHG44 cells. (**A**) The TMZ@UiO-66-NH_2 + ultrasound can inhibit migration of U251 and SHG44 cells, which was demonstrated by transwell assays. U251 and SHG44 cells that passed through the membrane were detected with crystal violet staining. (**B** and **C**) Data from experiments are presented in the form of histograms. (**D** and **E**) Western Blot analysis was carried out to detect the expression of MMP-2, MMP-9 and MMP-13 in U251 and SHG44 cells treated by PBS, TMZ, TMZ@UiO-66-NH_2 or TMZ@UiO-66-NH_2 + ultrasound. β-Actin was used for normalization. (**F**–**K**) Quantification of the protein levels of MMP-2, MMP-9 and MMP-13 in U251 and SHG44 cells. #Not Significant. *p<0.05, **p<0.01, ***p<0.001, ****p<0.0001. Data are expressed as means ± SDs (n=3).

Abbreviation: MMP, matrix metalloproteinase.

used to evaluate the apoptosis-inducing ability of U251 and SHG44 cells in the control group, TMZ group, UiO-66-NH2 nanocomposites group, and TMZ@UiO-66-NH_2 nanocomposites under the ultrasound group. The results showed that TMZ, TMZ@UiO-66-NH_2 nanocomposites and TMZ@UiO-66-NH_2 + ultrasound all could induce apoptosis compared with the Control, but the ability to promote apoptosis in the TMZ@UiO-66-NH_2 group was minimal based on flow cytometry (Figure 3B and C). From the results, we found that the percentage of apoptotic U251 cells grew from 11.6% to 53.4% after the administration of TMZ, and the apoptosis rate further increased to 66.6% in the TMZ@UiO-66-NH_2 +Ultrasound group. The apoptosis rates in the TMZ group and TMZ@UiO-66-NH2 +Ultrasound group of SHG44 cells were 58.2% and 71.1%, respectively, which were remarkably similar to those of U251 cells. In this analysis, treatment with TMZ@UiO-66-NH2 had a minor effect on inducing

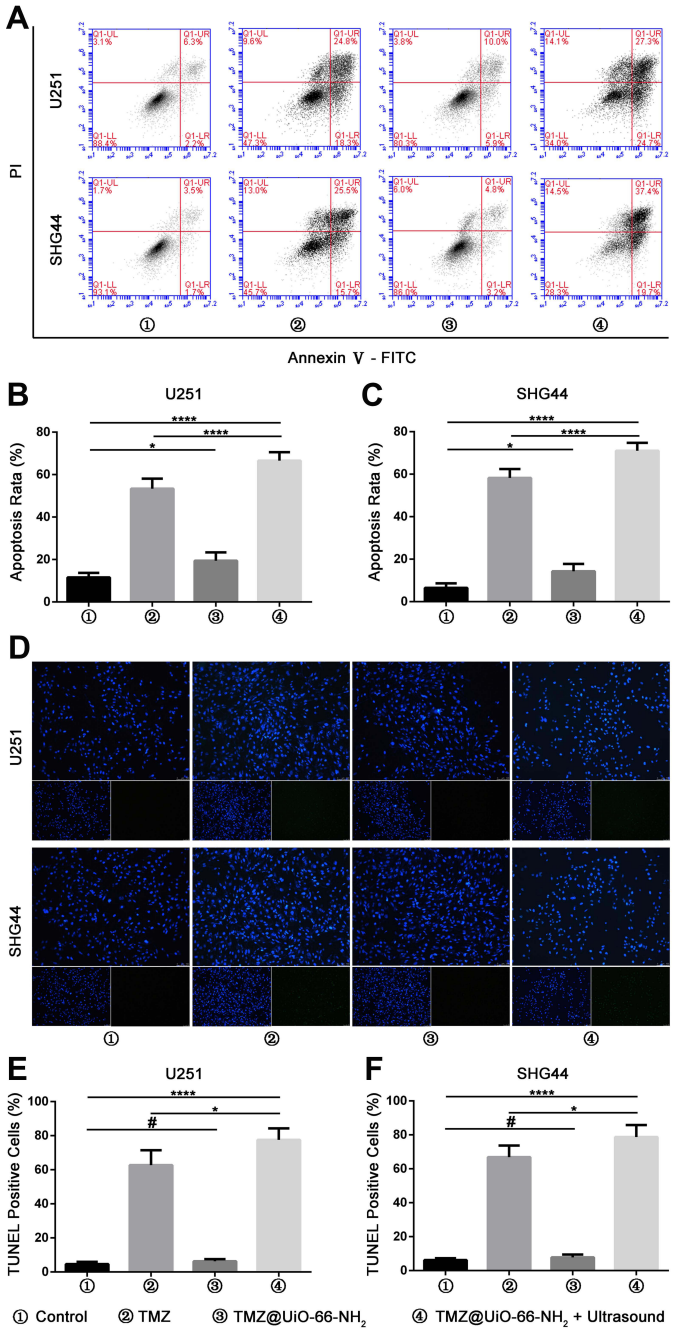

Figure 3 TMZ@UiO-66-NH_2 + ultrasound increased apoptotic rate in U251 and SHG44 cells. (**A**) Cells were treated by PBS, TMZ, TMZ@UiO-66-NH_2 or TMZ@UiO-66-NH_2 + ultrasound for 48 h, stained with PI and Annexin V-FITC, and analyzed by flow cytometry. (**B** and **C**) The percentage of the apoptotic cell population, which was analyzed by flow cytometry, was represented in the histograms. (**D**) TUNEL assay performed to assess the level of DNA damage and apoptosis of different groups (nuclei, blue; damaged DNA, green). (**E** and **F**) Quantification of percentage of TUNEL-positive cells. #Not Significant. *p<0.05, ****p<0.0001. Data are expressed as means ± SDs (n=3).

Abbreviations: DNA, deoxyribonucleic acid; PI, propidium iodide; FITC, fluorescein isothiocyanate; TUNEL, TdT-mediated dUTP nick end LIbeling.

glioma cell apoptosis compared with the control group due to insufficient drug release. The TUNEL assays results indicated the same situation (Figure 3E and F) and verified that the TMZ@UiO-66-NH2 +Ultrasound group had a significantly enhanced apoptosis effect on tumour cells compared with the other groups, even the TMZ group (Figure 3B, C, E and F). We further used a TUNEL assay to study the apoptosis of U251 and SHG44 cells at the DNA molecular level, and the general trend of the percentage of apoptotic cells was consistent with the results of flow cytometry analysis. The apoptosis induced by TMZ@UiO-66-NH_2+Ultrasound was higher than that

induced by TMZ, which was statistically significant in both U251 cells (77.6% to 66.7%, *p<0.05) and SHG44 cells (78.7% to 66.9%, *p<0.05). However, according to the results of the TUNEL assays, there were significant differences between the TMZ@(UiO-66-NH_2) and TMZ groups in both U251 cells and SHG44 cells, further confirming the slow drug release of TMZ@(UiO-66-NH_2). In contrast, TMZ raised the local drug concentration in a short period of time under ultrasonic shock and increased its conversion activity product MTIC (3-methyl-(triazine-1-) imidazole-4-formamide). MTIC plays a cytotoxic role by DNA mismatch repair of methylated adducts.[37] In addition, ultrasound waves can induce apoptosis of the tumour cell itself.[38] Increasing attention has been focussed on the role of ultrasound combined with chemotherapeutic agents in promoting glioma apoptosis.

Apoptosis is regulated by protein families such as the Bcl-2 family and the caspase family.[39] Previous studies have shown that glioma cells treated with TMZ exhibit changes in the expression levels of Bax and Bcl-2, which are involved in the mitochondrial pathway of apoptosis.[36] We selected the apoptosis-related proteins Bax, Bcl-2 and cleaved caspase-3 as the detection indices of the Western-blot experiments (Figure 4A and B). The ratio of Bax to Bcl-2 and cleaved caspase-3 in glioma cells induced by TMZ@UiO-66-NH_2 was, respectively,- higher than that in the Control group (*p<0.05), but lower than that in the TMZ group (Figure 4A–D). The index of TMZ@UiO-66-NH_2 + Ultrasound was stronger than that of the other groups. The ratios of Bax to Bcl-2 in U251 and SHG44 cells were 1.9 and 1.5 (Figure 4C and D), and the ratios of cleaved caspase-3 were 1.003 and 1.01 (Figure 4E and F). The possible mechanism of temozolomide combined with ultrasound underlying the synergistic effect at a molecular level is being examined. As reported in a previous study, these agents could inhibit the phosphoinositide 3-kinase (PI3K)/Akt/mammalian target of rapamycin (mTOR) pathway, followed by caspase 3-dependent apoptotic induction, which was characterized by the downregulation of antiapoptotic protein Bcl-2 and upregulation of the proapoptotic protein Bax and cleaved caspase-3.[40] The results demonstrated that the TMZ@UiO-66-NH_2 group could promote apoptosis compared with the control group, but the effect was weak, while the TMZ group and the TMZ@UiO-66-NH_2+Ultrasound group could effectively induce apoptosis, and the effect of promoting apoptosis in the TMZ@UiO-66-NH_2 +Ultrasound group was more obvious. The results further indicated that local region targeting and increased drug concentrations might enhance tumour cell apoptosis.

Then, we demonstrated that TMZ@UiO-66-NH_2 nanocomposites under ultrasound mainly killed tumour cells through TMZ rather than ultrasound in vitro. Previous results have verified that TMZ@UiO-66-NH_2 nanocomposites under ultrasound could kill malignant glioma cells by promoting apoptosis. In addition to apoptosis, migration and invasion, many studies have demonstrated that the proliferation of malignant glioma cells plays an important role in the lethality of glioma. Previous research has suggested that proliferation was tightly associated with the cell cycle, and the application of TMZ could induce significant G2/M arrest in malignant glioma cells. For example, Fu et al reported that temozolomide mainly causes tumour cells to stagnate at the G2/M stage by DNA methylation and mismatch repair failure.[41] Kanzawa et al investigated whether cell cycle arrest was induced in malignant glioma cells by TMZ by performing DNA flow cytometric analysis. TMZ treatment increased the population at the G2/M phase and decreased the population at the G1 phase in all malignant glioma cells they tested. These results indicated that TMZ induces G2/M arrest in malignant glioma cell lines.[42] For the reasons given above, we decided to detect the cell cycle under different treatment conditions to further explore the antitumour effect of TMZ@UiO-66-NH_2 under ultrasound. The cell cycle distribution of U251 cells and SHG44 cells was measured using a flow cytometry assay (Figure 5A). The results showed that both the TMZ and TMZ@UiO-66-NH_2 +Ultrasound groups could significantly interfere with the cell cycle, resulting in tumour cell stagnation at the G2/M stage. Additionally, TMZ@UiO-66-NH_2 nanocomposites under ultrasound could significantly induce G2/M arrest compared with the other groups in the quantitative analysis of cell cycle distribution (Figure 5B and C). When ultrasound and TMZ were applied together, the apoptotic rate and percentage of cells arrested at the G2/M stage were significantly higher compared with either treatment alone. TMZ could effectively decrease clonal and cellular growth with increased G2-M arrest by inducing autophagy via autophagy formation and p53 status.[42] When autophagy was prevented at an early stage, not only the characteristic pattern of LC3 localization but also the antitumor effect of TMZ was suppressed.[43] Therefore, the potential underlying mechanism may be related to autophagy, DNA methylation and mismatch repair failure.

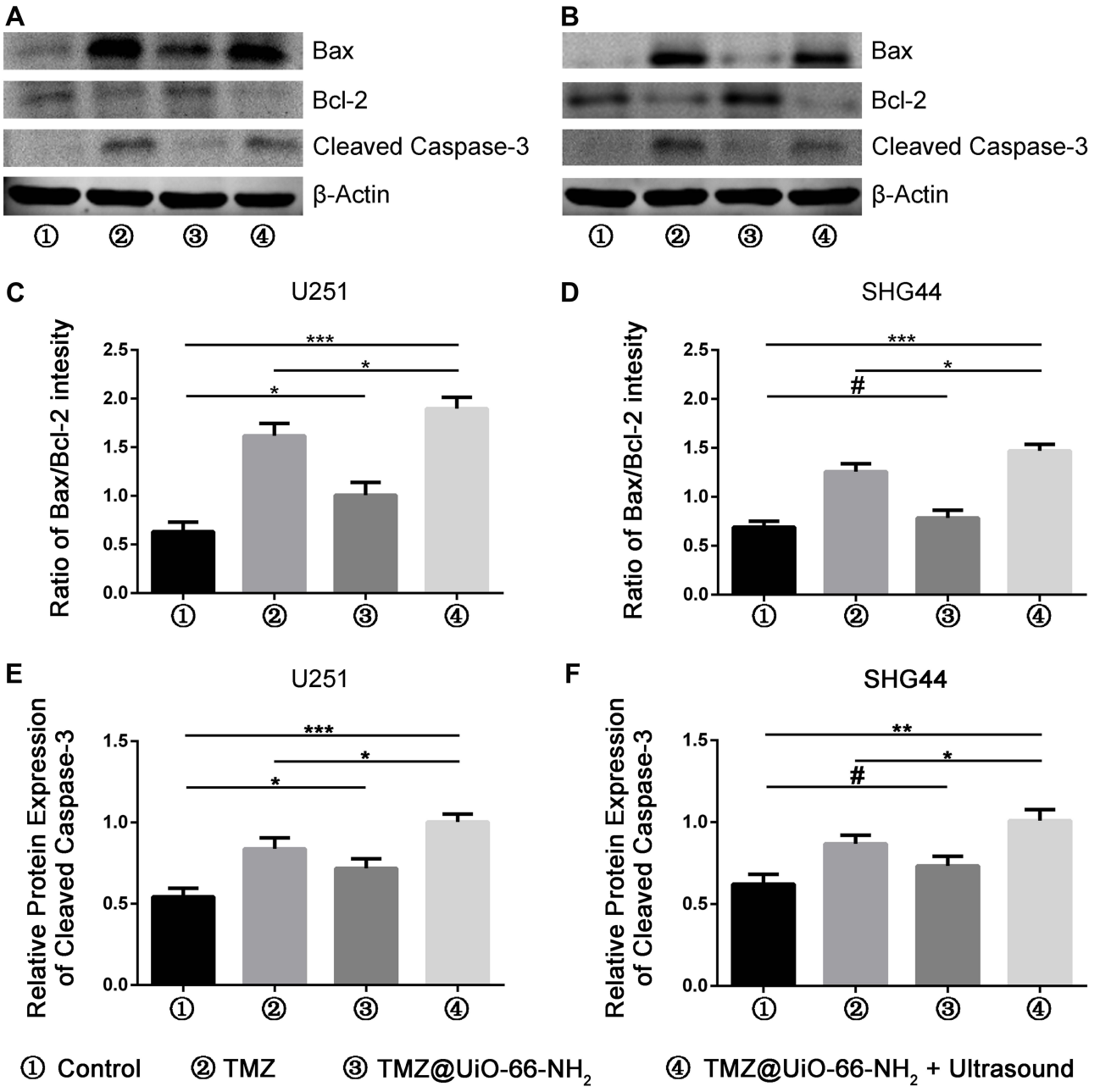

Figure 4 Western blots were applied to detect the expression of apoptosis-related proteins in U251 and SHG44 cells treated by PBS, TMZ, TMZ@UiO-66-NH_2 or TMZ@UiO-66-NH_2 + ultrasound for 48 h. (**A** and **B**) Western blot analysis showing that Bax, Bcl-2, cleaved caspase-3, and β-actin protein levels after different treatment. β-actin was used as a loading control. (**C**–**F**) Quantitative analysis of the Western blots was shown in histogram after being normalized by β-actin. Data were presented as the ratio of Bax to Bcl-2 and cleaved caspase-3. #Not significant. *p<0.05, **p<0.01, ***p<0.001. Data are expressed as means ± SDs (n=3).
Abbreviations: PBS, phosphate-buffered saline; TMZ, temozolomide.

Previous studies have confirmed a link between cell apoptosis and G2/M arrest in malignant glioma cells under TMZ treatment. TMZ can induce DNA damage-triggered mismatch in the G2/M phase, which can cause apoptosis and G2/M arrest simultaneously. In our study, we not only found a more significant G2/M arrest under treatment with TMZ@UiO-66-NH_2 +Ultrasound than TMZ alone but also a higher apoptosis rate compared with TMZ under identical experimental conditions, Thus, we speculated that the application of TMZ@UiO-66-NH2+Ultrasound was more effective compared with TMZ alone in the treatment of malignant glioma. As shown in Figure 5A, glioma cells mainly exhibit cell cycle disorders caused by TMZ to induce apoptosis.

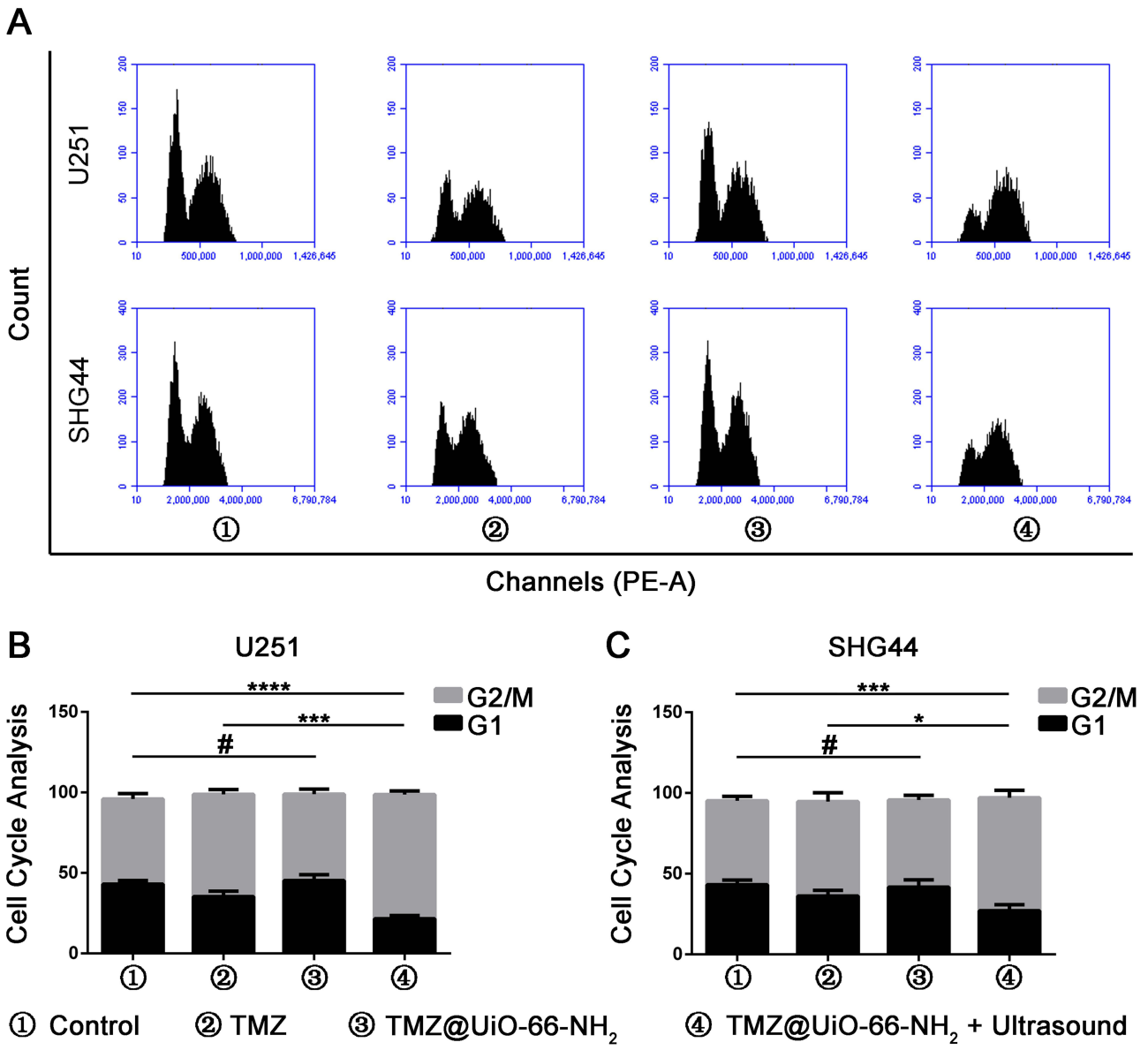

Figure 5 Combination treatment with TMZ@UiO-66-NH_2 and ultrasound arrested U251 and SHG44 cells cycle in G2/M phase. (**A**) Flow cytometry analysis of U251 and SHG44 cells with PI staining for cell cycle status in different groups. (**B** and **C**) Histograms represents the quantitative analysis of cell cycle distribution. #Not significant. *p<0.05, ***p<0.001, ****p<0.0001. Data are expressed as means ± SDs (n=3).

Abbreviations: TMZ, temozolomide; MOF, metal organic frameworks; PI, propidium iodide.

To verify the biological safety of TMZ@UiO-66-NH_2 nanocomposites, histological analysis of the liver, heart, spleen, lung and kidney tissue of various tissue slices from mice was conducted 4 weeks after the indicated treatments (Figure 6A). There was no significant organ structure or cell damage between the TMZ@UiO-66-NH_2 and control groups. The observed excellent biocompatibility may have contributed to the completely effective degradation of UiO-66-NH_2 into ions and organic molecules and excretion by the body.[44] Additionally, our previous results have shown that TMZ loaded in TMZ@UiO-66-NH_2 nanocomposites has the advantage of few leakage in normal tissue, resulting in lower toxicity.

As verified by a number of studies, TMZ can induce glioma cells to undergo apoptosis, autophagy and senescence; however, TMZ-induced side effects and drug tolerance to human gliomas remain challenging issues. Long-term and high-dose TMZ treatment may lead to significant bone marrow suppression and liver damage.[41] Through in vivo experiments, we verified that the side effects of temozolomide alone were obvious. However, after TMZ@UiO-66-NH_2 nanocomposite treatment, bone

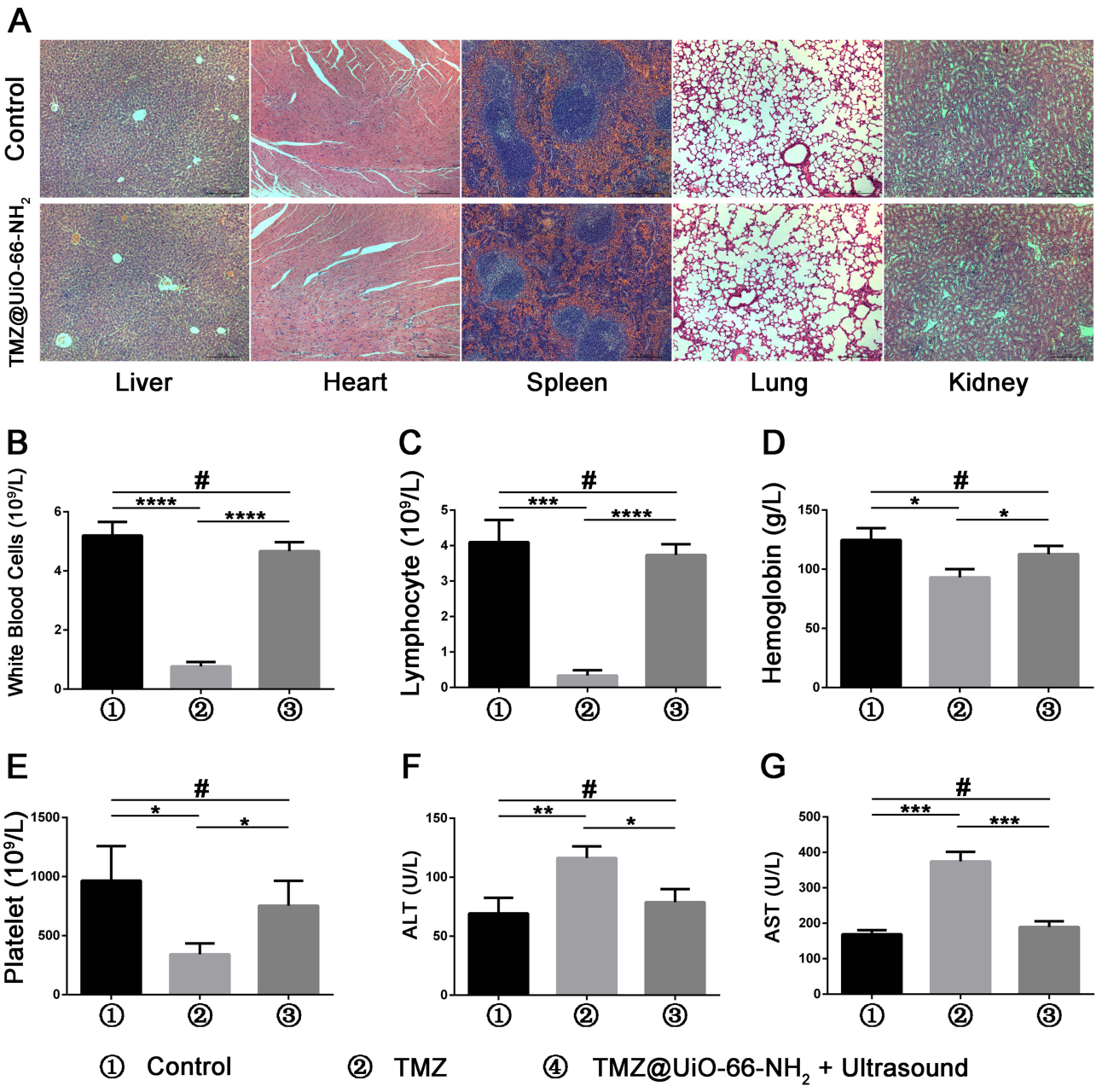

Figure 6 Verification of the biosafety of TMZ@UiO-66-NH_2. (**A**) Histological analysis of the liver, heart, spleen, lung and kidney tissue of various tissue slices from mice at 4 weeks after indicated treatments. There were no significant differences between the TMZ@UiO-66-NH_2 and control groups that indicated the safety of TMZ@UiO-66-NH_2. (**B**–**E**) Quantitative analysis of the myelosuppression markers, white blood cell, lymphocyte, hemoglobin and platelet, are shown in the form of histograms. (**F** and **G**) Quantitative analysis of the serum liver function markers, ALT and AST, are shown in the form of histograms. #Not significant. *p<0.05, **p<0.01, ***p<0.001, ****p<0.0001. Data are expressed as means ± SDs (n=3).

Abbreviations: TMZ, temozolomide; MOF, metal organic frameworks; ALT, alanine aminotransferase; AST, aspartate transaminase.

marrow suppression and liver enzyme indices of nude mice remained stable compared with those of the control group (Figure 6B–G). In addition, TMZ can be effectively encapsulated and released at a proper concentration, which reduces the side effects of the drug.

Furthermore, we determined the anti-tumour efficacy of TMZ@UiO-66-NH_2 after ultrasound in vivo. The results showed that the malignant glioma of mice injected with PBS or TMZ@UiO-66-NH_2 grew rapidly, and the tumour volume was slightly reduced with the administration of TMZ. Interestingly, treatment with TMZ@UiO-66-NH_2 + ultrasound effectively inhibited malignant glioma growth, which was better than the TMZ group (Figure 7A and B). The tumour volumes and weights of the TMZ@UiO-66-NH_2

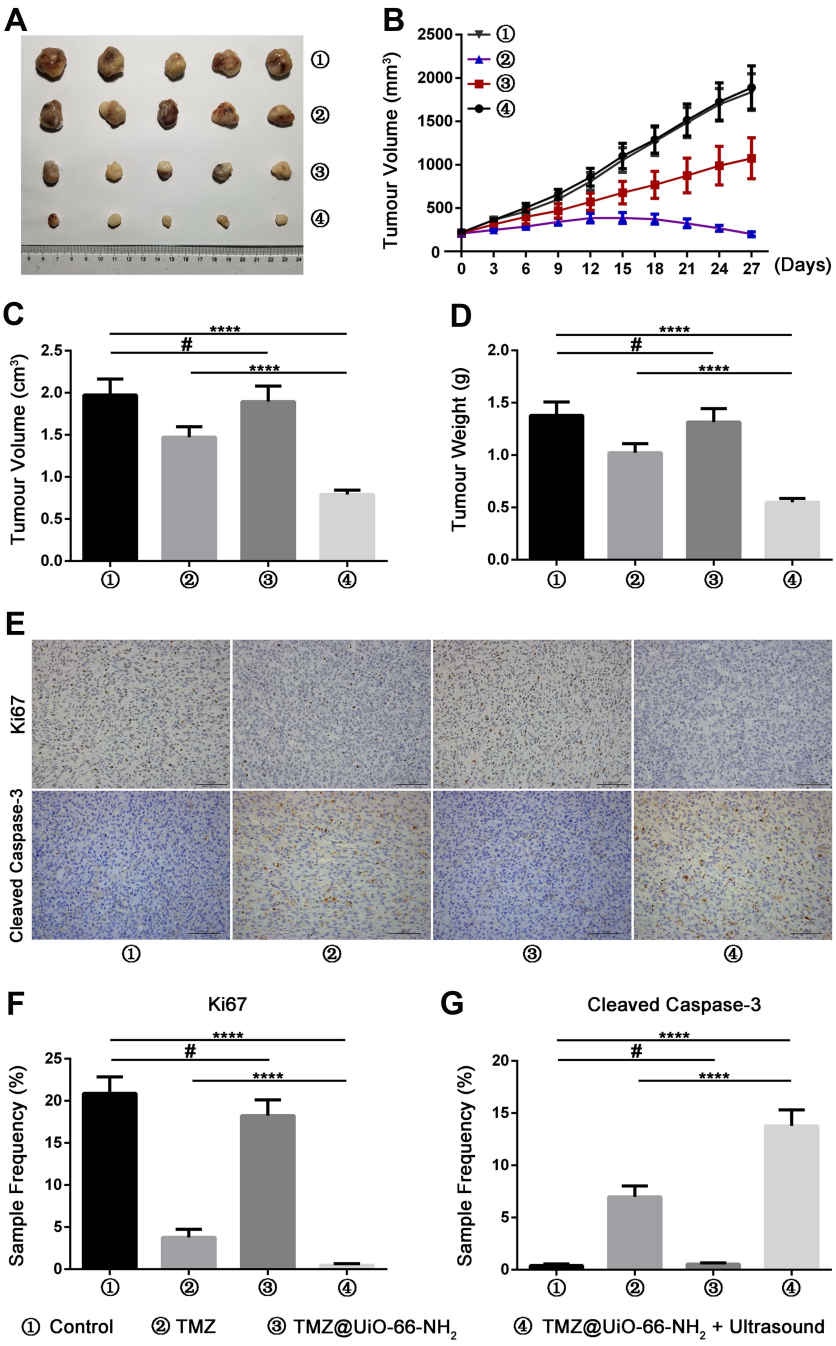

Figure 7 Combination treatment with TMZ@UiO-66-NH_2 and ultrasound improve therapeutic outcome in glioblastoma. (**A**) Photographs of tumors that developed in neuroglioma nude mice tumor model after injection of U87 cells. (**B**) The growth curve of U87 cells derived subcutaneous tumor xenografts after different treatments. (**C** and **D**) Graphs presenting final tumor volume and weight in different groups. (**E**) Representative pictures of cleaved caspase-3 and Ki-67 immunohistochemical staining in derived tumor xenograft at different groups (scale bars: 100 μm, 400×magnification). (**F** and **G**) Quantitative analysis of the sample frequency of cleaved caspase-3 and Ki-67 immunoactivity in neuroglioma nude mice tumor model of different groups. #Not significant. ****p<0.0001. Data are expressed as means ± SDs (n=3).
Abbreviations: TMZ, temozolomide; MOF, metal organic frameworks.

nanocomposites under ultrasound were significantly reduced compared with those in the TMZ@UiO-66-NH_2 nanocomposite and TMZ groups (Figure 7C and D). On the one hand, the drug-loaded nanoparticles could be fully released under ultrasonic shock, and the local concentration was greatly increased. It has been shown that delivery of a targeted ultrasonic wave causes an interaction between the administered microbubbles and the capillary bed resulting in enhanced vessel permeability.[13] On the other hand, ultrasound has the advantage of transiently disrupting the BBB

allowing improved drug delivery to the brain.[9,45] Indicating that ultrasound delivery of temozolomide across the BBB is a feasible and effective treatment for glioma.

To verify the tumour inhibition mechanism of the in vivo tumour bearing experiment, we collected the tumour tissue from each group for immunohistochemical detection, and we selected Ki67 and cleaved caspase-3 as the detection indices (Figure 7E). The results showed that the expression of tumour Ki67 in the TMZ and TMZ@UiO-66-NH_2 + Ultrasound groups was significantly lower than that in the control and TMZ@UiO-66-NH_2 groups, while the expression of tumour cleaved caspase-3 was significantly higher (Figure 7F–G). Temozolomide cytotoxicity is mainly manifested in the alkylation of the guanine sixth oxygen atom and seventh nitrogen atom on the DNA molecule. Through mismatch repair of methylated adducts, the cycle of glioma cells is affected, thus the cytotoxic effect is triggered[46] as demonstrated in the results. Moreover, the inhibitory effect in the TMZ@UiO-66-NH_2 + Ultrasound group was more obvious than that in the II group (Figure 7E–G). Ultrasound may induce cell death by strengthening the induction of apoptosis and inhibiting invasion. Studies have demonstrated that high-intensity focused ultrasound can produce mainly necrosis of the tumour tissue in the focus area and induce apoptosis of the tumour cells in the perifocus area around the tumour periphery. Additionally, the proliferative activity of the entire tumour is markedly decreased.[38]

Throughout the experiment, we verified optimistic results in vitro cell experiments and in vivo subcutaneous tumor-bearing model. In the next step, orthotopic model of glioblastoma experiments would be carried out to verify the effect of BBB penetration. Ultrasound combined with MOF vehicle has great potential for glioma treatment. A clinical application design such as tumor site skull removal or skull tumor lesions reserved ultrasound probe can be further developed, which makes the application of ultrasound daily a reality. The ultrasonic apparatus is suitable for moving and hand-held operation. Therefore, ultrasound mediated-drug targeted release can significantly reduce the toxic side effects of TMZ and improve the prognosis of malignant glioma.

Conclusions

TMZ displayed high cytotoxicity against glioma, yet this efficacy was not satisfactory. In this study, we developed TMZ@UiO-66-NH_2 nanocomposites, which could be well delivered into the tumor tissue and exhibit excellent biocompatibility and biosafety. The TMZ were dramatically released in the tumor site under ultrasound to reach enhanced antitumor effect. Our results suggested that ultrasound-directed TMZ@UiO-66-NH_2 nanocomposites have great potential as a safe and effective method of treatment with enhanced therapeutic effect and reduced side effect.

Acknowledgments

This study was funded by Shanghai Natural Science Foundation (grant No.18ZR1434500), Shanghai Lead Project Foundation (grant No.18411962500), Shanghai Natural Science Foundation (grant No.19ZR1448900).

Disclosure

The authors report no conflicts of interest in this work.

References

1. Ostrom QT, Gittleman H, Truitt G, et al. CBTRUS statistical report: primary brain and other central nervous system tumors diagnosed in the United States in 2011–2015. *Neuro Oncol*. 2018;20(suppl_4):iv1–iv86. doi:10.1093/neuonc/noy131
2. Vaios EJ, Nahed BV, Muzikansky A, Fathi AT, Dietrich J. Bone marrow response as a potential biomarker of outcomes in glioblastoma patients. *J Neurosurg*. 2017;127(1):132–138. doi:10.3171/2016.7.JNS16609
3. Majumder J, Taratula O, Minko T. Nanocarrier-based systems for targeted and site specific therapeutic delivery. *Adv Drug Deliv Rev*. 2019;144:57–77.
4. Zahid M, Zhang D, Xu X, Pan M, Reda AT, Xu W. Barbituric and thiobarbituric acid-based UiO-66-NH2 adsorbents for iodine gas capture: characterization, efficiency and mechanisms. *J Hazard Mater*. 2021;416:125835. doi:10.1016/j.jhazmat.2021.125835
5. Wu MX, Yang YW. Metal-Organic Framework (MOF)-based drug/cargo delivery and cancer therapy. *Adv Mater*. 2017;29(23):1606134. doi:10.1002/adma.201606134
6. Abanades Lazaro I, Haddad S, Rodrigo-Munoz JM, et al. Surface-functionalization of Zr-Fumarate MOF for selective cytotoxicity and immune system compatibility in nanoscale drug delivery. *ACS Appl Mater Interfaces*. 2018;10(37):31146–31157. doi:10.1021/acsami.8b11652
7. Wang Y, Zhao Q, Han N, et al. Mesoporous silica nanoparticles in drug delivery and biomedical applications. *Nanomedicine*. 2015;11(2):313–327. doi:10.1016/j.nano.2014.09.014
8. Wang Y, Bi K, Shu J, et al. Ultrasound-controlled DOX-SiO 2 nanocomposites enhance the antitumour efficacy and attenuate the toxicity of doxorubicin. *Nanoscale*. 2019;11(10):4210–4218. doi:10.1039/C8NR08497A
9. Zhang DY, Dmello C, Chen L, et al. Ultrasound-mediated delivery of paclitaxel for glioma: a comparative study of distribution, toxicity, and efficacy of albumin-bound versus cremophor formulations. *Clin Cancer Res*. 2020;26(2):477–486. doi:10.1158/1078-0432.CCR-19-2182
10. Beccaria K, Canney M, Goldwirt L, et al. Ultrasound-induced opening of the blood-brain barrier to enhance temozolomide and irinotecan delivery: an experimental study in rabbits. *J Neurosurg*. 2016;124(6):1602–1610. doi:10.3171/2015.4.JNS142893
11. Mainprize T, Lipsman N, Huang Y, et al. Blood-brain barrier opening in primary brain tumors with non-invasive MR-guided focused ultrasound: a clinical safety and feasibility study. *Sci Rep*. 2019;9(1):321. doi:10.1038/s41598-018-36340-0

12. Wu S-Y, Aurup C, Sanchez CS, et al. Efficient blood-brain barrier opening in primates with neuronavigation-guided ultrasound and real-time acoustic mapping. *Sci Rep*. 2018;8(1):7978. doi:10.1038/s41598-018-25904-9
13. Alli S, Figueiredo CA, Golbourn B, et al. Brainstem blood brain barrier disruption using focused ultrasound: a demonstration of feasibility and enhanced doxorubicin delivery. *J Control Release*. 2018;281:29–41. doi:10.1016/j.jconrel.2018.05.005
14. Guo Y, Lee H, Fang Z, et al. Single-cell analysis reveals effective siRNA delivery in brain tumors with microbubble-enhanced ultrasound and cationic nanoparticles. *Sci Adv*. 2021;7(18):eabf7390. doi:10.1126/sciadv.abf7390
15. Jamshidifard S, Koushkbaghi S, Hosseini S, et al. Incorporation of UiO-66-NH2 MOF into the PAN/chitosan nanofibers for adsorption and membrane filtration of Pb(II), Cd(II) and Cr(VI) ions from aqueous solutions. *J Hazard Mater*. 2019;368:10–20. doi:10.1016/j.jhazmat.2019.01.024
16. Karim R, Palazzo C, Evrard B, Piel G. Nanocarriers for the treatment of glioblastoma multiforme: current state-of-the-art. *J Control Release*. 2016;227:23–37. doi:10.1016/j.jconrel.2016.02.026
17. Bao T, Fu R, Wen W, Zhang X, Wang S. Target-driven cascade-amplified release of loads from DNA-gated metal-organic frameworks for electrochemical detection of cancer biomarker. *ACS Appl Mater Interfaces*. 2020;12(2):2087–2094. doi:10.1021/acsami.9b18805
18. Crake A, Christoforidis KC, Kafizas A, Zafeiratos S, Petit C. CO_2 capture and photocatalytic reduction using bifunctional TiO 2 /MOF nanocomposites under UV-vis irradiation. *Appl Catal B*. 2017;210:131–140. doi:10.1016/j.apcatb.2017.03.039
19. Hu J, Wang J, Wang G, Yao Z, Dang X. Pharmacokinetics and antitumor efficacy of DSPE-PEG2000 polymeric liposomes loaded with quercetin and temozolomide: analysis of their effectiveness in enhancing the chemosensitization of drug-resistant glioma cells. *Int J Mol Med*. 2016;37(3):690–702. doi:10.3892/ijmm.2016.2458
20. Horcajada P, Chalati T, Serre C, et al. Porous metal-organic-framework nanoscale carriers as a potential platform for drug delivery and imaging. *Nat Mater*. 2010;9(2):172–178. doi:10.1038/nmat2608
21. Kaneko OF, Willmann JK. Ultrasound for molecular imaging and therapy in cancer. *Quant Imaging Med Surg*. 2012;2(2):87–97.
22. Mitragotri S. Healing sound: the use of ultrasound in drug delivery and other therapeutic applications. *Nat Rev Drug Discov*. 2005;4(3):255–260. doi:10.1038/nrd1662
23. Liberman A, Wang J, Lu N, et al. Mechanically tunable hollow silica ultrathin nanoshells for ultrasound contrast agents. *Adv Funct Mater*. 2015;25(26):4049–4057. doi:10.1002/adfm.201500610
24. Mesiwala AH, Farrell L, Wenzel HJ, et al. High-intensity focused ultrasound selectively disrupts the blood-brain barrier in vivo. *Ultrasound Med Biol*. 2002;28(3):389–400. doi:10.1016/S0301-5629(01)00521-X
25. Hynynen K, McDannold N, Sheikov NA, Jolesz FA, Vykhodtseva N. Local and reversible blood-brain barrier disruption by noninvasive focused ultrasound at frequencies suitable for trans-skull sonications. *Neuroimage*. 2005;24(1):12–20. doi:10.1016/j.neuroimage.2004.06.046
26. Zhou K, Zhang C, Yao H, et al. Knockdown of long non-coding RNA NEAT1 inhibits glioma cell migration and invasion via modulation of SOX2 targeted by miR-132. *Mol Cancer*. 2018;17(1):105. doi:10.1186/s12943-018-0849-2
27. Smith SJ, Tyler BM, Gould T, et al. Overall survival in malignant glioma is significantly prolonged by neurosurgical delivery of etoposide and temozolomide from a thermo-responsive biodegradable paste. *Clin Cancer Res*. 2019;25(16):5094–5106. doi:10.1158/1078-0432.CCR-18-3850
28. Tian Y, Liu Z, Tan H, et al. New aspects of ultrasound-mediated targeted delivery and therapy for cancer. *Int J Nanomedicine*. 2020;15:401–418. doi:10.2147/IJN.S201208
29. Du M, Chen Z, Chen Y, Li Y. Ultrasound-targeted delivery technology: a novel strategy for tumor- targeted therapy. *Curr Drug Targets*. 2019;20(2):220–231. doi:10.2174/1389450119666180731095441
30. Kondraganti S, Mohanam S, Chintala SK, et al. Selective suppression of matrix metalloproteinase-9 in human glioblastoma cells by antisense gene transfer impairs glioblastoma cell invasion. *Cancer Res*. 2000;60(24):6851–6855.
31. Marin-Ramos NI, Thein TZ, Cho HY, et al. NEO212 inhibits migration and invasion of glioma stem cells. *Mol Cancer Ther*. 2018;17(3):625–637. doi:10.1158/1535-7163.MCT-17-0591
32. Bi Y, Li H, Yi D, et al. Cordycepin augments the chemosensitivity of human glioma cells to temozolomide by activating AMPK and inhibiting the AKT signaling pathway. *Mol Pharm*. 2018;15(11):4912–4925. doi:10.1021/acs.molpharmaceut.8b00551
33. Ni Q, Fan Y, Zhang X, Fan H, Li Y. In vitro and in vivo study on glioma treatment enhancement by combining temozolomide with calycosin and formononetin. *J Ethnopharmacol*. 2019;242:111699. doi:10.1016/j.jep.2019.01.023
34. Yuan Y, Xue X, Guo RB, Sun XL, Hu G. Resveratrol enhances the antitumor effects of temozolomide in glioblastoma via ROS-dependent AMPK-TSC-mTOR signaling pathway. *CNS Neurosci Ther*. 2012;18(7):536–546. doi:10.1111/j.1755-5949.2012.00319.x
35. Karpel-Massler G, Pareja F, Aime P, et al. PARP inhibition restores extrinsic apoptotic sensitivity in glioblastoma. *PLoS One*. 2014;9(12):e114583. doi:10.1371/journal.pone.0114583
36. Das A, Banik NL, Patel SJ, Ray SK. Dexamethasone protected human glioblastoma U87MG cells from temozolomide induced apoptosis by maintaining Bax: Bcl-2 ratio and preventing proteolytic activities. *Mol Cancer*. 2004;3(1):36. doi:10.1186/1476-4598-3-36
37. Yang Z, Wei D, Dai X, et al. C8-substituted imidazotetrazine analogs overcome temozolomide resistance by inducing DNA adducts and DNA damage. *Front Oncol*. 2019;9:485. doi:10.3389/fonc.2019.00485
38. Suehiro S, Ohnishi T, Yamashita D, et al. Enhancement of antitumor activity by using 5-ALA-mediated sonodynamic therapy to induce apoptosis in malignant gliomas: significance of high-intensity focused ultrasound on 5-ALA-SDT in a mouse glioma model. *J Neurosurg*. 2018;129(6):1416–1428. doi:10.3171/2017.6.JNS162398
39. Gross A, McDonnell JM, Korsmeyer SJ. BCL-2 family members and the mitochondria in apoptosis. *Genes Dev*. 1999;13(15):1899–1911. doi:10.1101/gad.13.15.1899
40. Xu H, Jia F, Singh PK, et al. Synergistic anti-glioma effect of a coloaded nano-drug delivery system. *Int J Nanomed*. 2017;12:29–40. doi:10.2147/IJN.S116367
41. Fu W, You C, Ma L, et al. Enhanced efficacy of temozolomide loaded by a tetrahedral framework DNA nanoparticle in the therapy for glioblastoma. *ACS Appl Mater Interfaces*. 2019;11(43):39525–39533. doi:10.1021/acsami.9b13829
42. Kanzawa T, Germano IM, Komata T, et al. Role of autophagy in temozolomide-induced cytotoxicity for malignant glioma cells. *Cell Death Differ*. 2004;11(4):448–457. doi:10.1038/sj.cdd.4401359
43. Lee SW, Kim HK, Lee NH, et al. The synergistic effect of combination temozolomide and chloroquine treatment is dependent on autophagy formation and p53 status in glioma cells. *Cancer Lett*. 2015;360(2):195–204. doi:10.1016/j.canlet.2015.02.012
44. Morris W, Briley WE, Auyeung E, Cabezas MD, Mirkin CA. Nucleic acid-metal organic framework (MOF) nanoparticle conjugates. *J Am Chem Soc*. 2014;136(20):7261–7264. doi:10.1021/ja503215w
45. Shen Y, Pi Z, Yan F, et al. Enhanced delivery of paclitaxel liposomes using focused ultrasound with microbubbles for treating nude mice bearing intracranial glioblastoma xenografts. *Int J Nanomed*. 2017;12:5613–5629. doi:10.2147/IJN.S136401
46. Renziehausen A, Tsiailanis AD, Perryman R, et al. Encapsulation of temozolomide in a calixarene nanocapsule improves its stability and enhances its therapeutic efficacy against glioblastoma. *Mol Cancer Ther*. 2019;18(9):1497–1505. doi:10.1158/1535-7163.MCT-18-1250